


Pathogenic variants of the coenzyme A biosynthesis-associated enzyme phosphopantothenoylcysteine decarboxylase cause autosomal-recessive dilated cardiomyopathy

Irene Bravo-Alonso¹ | Matías Morin^{2,3} | Laura Arribas-Carreira¹ |
 Mar Álvarez¹ | Consuelo Pedrón-Giner⁴ | Lucia Soletto² | Carlos Santolaria⁵ |
 Santiago Ramón-Maiques⁶ | Magdalena Ugarte¹ | Pilar Rodríguez-Pombo¹ |
 Joaquín Ariño⁵ | Miguel Ángel Moreno-Pelayo^{2,3} | Belén Pérez¹ 

¹Centro de Diagnóstico de Enfermedades Moleculares, Centro de Biología Molecular, Universidad Autónoma de Madrid, CIBERER, IdiPAZ, Madrid, Spain

²Servicio de Genética, Hospital Universitario Ramón y Cajal, IRYCIS, Madrid, Spain

³Centro de Investigación Biomédica en Red de Enfermedades Raras, Instituto de Salud Carlos III (CB06/07/0048; CIBERER-ISCI), Madrid, Spain

⁴Sección de Gastroenterología y Nutrición, Hospital Infantil Universitario Niño Jesús, Madrid, Spain

⁵Institut de Biotecnologia i Biomedicina & Departament de Bioquímica i Biologia Molecular, Universitat Autònoma de Barcelona, Cerdanyola del Vallès, Spain

⁶Instituto de Biomedicina de Valencia (IBV) CSIC. CIBERER., Valencia, Spain

Correspondence

Belén Pérez, Centro de Diagnóstico de Enfermedades Moleculares, Centro de Biología Molecular, Universidad Autónoma de Madrid, CIBERER, IdiPAZ, Madrid 28049, Spain.
 Email: belen.perez@uam.es

Abstract

Coenzyme A (CoA) is an essential cofactor involved in a range of metabolic pathways including the activation of long-chain fatty acids for catabolism. Cells synthesize CoA de novo from vitamin B5 (pantothenate) via a pathway strongly conserved across prokaryotes and eukaryotes. In humans, it involves five enzymatic steps catalyzed by four enzymes: pantothenate kinase (PANK [isoforms 1–4]), 4'-phosphopantothenoylcysteine synthetase (PPCS), phosphopantothenoylcysteine decarboxylase (PPCDC), and CoA synthase (COASY). To date, inborn errors of metabolism associated with all of these genes, except *PPCDC*, have been described, two related to neurodegeneration with brain iron accumulation (NBIA), and one associated with a cardiac phenotype. This paper reports another defect in this pathway (detected in two sisters), associated with a fatal cardiac phenotype, caused by biallelic variants (p.Thr53Pro and p.Ala95Val) of *PPCDC*. *PPCDC* enzyme (EC 4.1.1.36) catalyzes the decarboxylation of 4'-phosphopantothenoylcysteine to 4'-phosphopantetheine in CoA biosynthesis. The variants p.Thr53Pro and p.Ala95Val affect residues highly conserved across different species; p.Thr53Pro is involved in the binding of flavin mononucleotide, and p.Ala95Val is likely a destabilizing mutation. Patient-derived fibroblasts showed an absence of *PPCDC* protein, and nearly 50% reductions in CoA levels. The cells showed clear energy deficiency problems, with defects in mitochondrial respiration, and mostly glycolytic ATP synthesis. Functional studies performed in yeast suggest these mutations to be

Irene Bravo-Alonso and Matías Morin are co-authors.

Joaquín Ariño, Miguel Ángel Moreno-Pelayo, and Belén Pérez are senior authors.

This is an open access article under the terms of the [Creative Commons Attribution-NonCommercial](https://creativecommons.org/licenses/by-nc/4.0/) License, which permits use, distribution and reproduction in any medium, provided the original work is properly cited and is not used for commercial purposes.

© 2022 The Authors. *Journal of Inherited Metabolic Disease* published by John Wiley & Sons Ltd on behalf of SSIEM.

Funding information

Consejería de Educación, Juventud y Deporte, Comunidad de Madrid, Grant/Award Number: B2017/BMD3721; Instituto de Salud Carlos III, Grant/Award Number: PI19/01155; Ministerio de Economía, Industria y Competitividad, Grant/Award Number: BFU2017-82574-P

Communicating Editor: D. Sean Froese

functionally relevant. In summary, this work describes a new, ultra-rare, severe inborn error of metabolism due to pathogenic variants of *PPCDC*.

KEYWORDS

biosynthesis of coenzyme A, dilated cardiomyopathy, inborn errors of metabolism, *PPCDC*

1 | INTRODUCTION

Coenzyme A (CoA) is an essential cofactor involved in approximately 9% of metabolic reactions.¹ It is synthesized de novo via a pathway strongly conserved across prokaryotes and eukaryotes. This involves five steps catalyzed by the enzymes pantothenate kinase (PANK—for which, in mammals, four gene-encoded isoforms have been described: PANK1, PANK2, PANK3, and PANK4), 4'-phosphopantothenoylcysteine synthetase (PPCS), phosphopantothenoylcysteine decarboxylase (PPCDC), and 4'-phosphopantetheine adenylyltransferase (PPAT) and dephosphoCoA kinase (DPCK)—which in humans is a bifunctional enzyme known as CoA synthase (COASY)² (Figure 1).

Eukaryotic cells obtain CoA via the uptake of extracellular precursors, especially vitamin B5, which is then converted into CoA. However, an alternative mechanism has been described that allows low intracellular CoA levels to be compensated via the use of exogenous CoA. In mice, *Caenorhabditis elegans* and *Drosophila melanogaster*, extracellular CoA is directly converted into 4'-phosphopantetheine via the action of ectonucleotide pyrophosphatases (ENPPs)^{3,5} (Figure 1). 4'-phosphopantetheine is stable in serum and can be translocated via passive diffusion. Inside the cell, it is reconverted into CoA by COASY.

Defects in three of the four genes involved in the canonical CoA synthesis pathway have been described in mammals. Pathogenic variants in *PANK2*^{6,7} (MIM#606157) and *COASY*⁸ (MIM#609855) cause a neurodegenerative phenotype associated with brain iron accumulation (NBIA).⁹ Surprisingly, the phenotype described in the two families reported with pathogenic variants of *PPCS* (MIM#609853), involved a cardiac phenotype and the absence of any neurodegeneration.¹⁰ *PPCDC* encodes a cysteine decarboxylase that uses flavin mononucleotide (FMN) as a cofactor¹¹ and is the only gene in this pathway yet to be associated with human disease. *PPCDC* (EC 4.1.1.36) catalyzes the decarboxylation of 4'-phosphopantothenoylcysteine to 4'-phosphopantetheine. In humans, the native form is a predominantly cytosolic, 204 amino acid homotrimer (Uniprot, GeneCards, and Human Protein Atlas).

When defects are described in a gene for the first time, functional analysis is required to demonstrate their clinical effects. This can be performed in patient-derived fibroblasts, cellular models of disease generated by gene editing, and other models. Yeasts also offer, in many cases, an excellent model system.¹² In the present work, *Saccharomyces cerevisiae* was used as a model organism to test the functional effects of *PPCDC* variants identified in two patients who were sisters. In *S. cerevisiae* and related yeasts, *PPCDC* is an unusual heterotrimer composed of a necessary subunit, Cab3 (Ykl088W), plus two Hal3 or Vhs3 subunits (or a combination of both).¹³ The catalytic site is formed at the interface of the Hal3/Vhs3 and Cab3 monomers; Cab3 provides the catalytic Cys478 residue, and Hal3 (or Vhs3) the crucial His378 (459 in Vhs3) residue. *CAB3* is thus an essential gene, and concurrent mutations in *HAL3* and *VHS3* result in a lethal phenotype. Hal3 and Vhs3 are moonlighting proteins since they are also negative regulatory subunits of the Ppz1 protein phosphatase,^{14,15} and thus affect salt tolerance and the cell cycle.^{16–18}

This work describes the detection of two patients from a non-consanguineous family with variants in *PPCDC*, the only gene involved in CoA synthesis for which pathogenic variants have not yet been described. Two different models, patient-derived fibroblast, and the yeast *S. cerevisiae*, were used to demonstrate the pathogenic effect of these variants: an ultra-rare, fatal, inborn error of metabolism associated with cardiomyopathy.

2 | PATIENTS AND METHODS

The work adhered to the Declaration of Helsinki and was approved by the Ethics Committee of the *Universidad Autónoma de Madrid* (CEI-105-2052). Informed written consent to be included in the study was obtained from the patient's parents.

2.1 | Patients

The study patients were two sisters (P1 and P2) from a non-consanguineous family. P1, the firstborn daughter, debuted

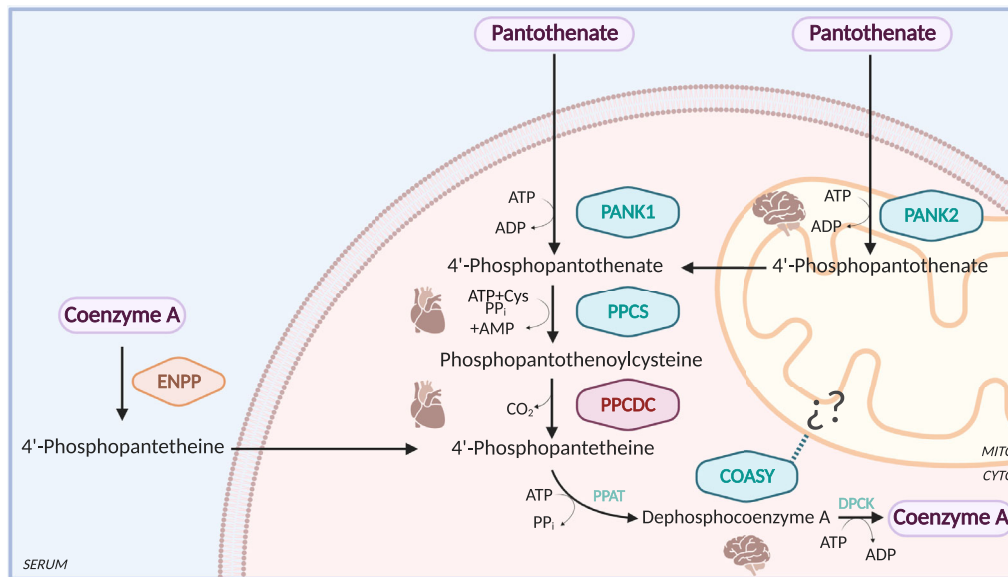


FIGURE 1 Coenzyme A synthesis and alternative pathways. Subcellular localization of the PANK2, PPCS, PPCDC, and COASY proteins, and the alternative route of incorporation of 4'-phosphopantetheine.³ COASY has been localized in the outer mitochondrial membrane, in the mitochondrial matrix, and in the nucleus.⁴ The brain or heart is the most commonly affected tissue related to each gene defect (see cartoons). CYTO, cytoplasm; MITO, mitochondria; SERUM, cell medium with serum.

at just 2 days of age with lactic acidosis (HP:0003128), hyperammonemia (HP:0001987), hypertransaminemia (HP:0002910), and elevated creatine kinase (HP:0003236). She showed neurological involvement with lethargy (HP:0001254), a tendency to opisthotonus (HP:0002179), axial hypotonia (HP:0009062), hypertonia of the four limbs (HP:0002509), genu valgum feet (HP:0002857), hip dysplasia (HP:0001385), a triangular face (HP:0000325), micrognathia (HP:0000347), swallowing difficulties (HP:0002015), and dilated cardiomyopathy (HP:0001644). Biochemical analysis in body fluids revealed hypoglycemia (HP:0001943), ketonuria (HP:0002919), alanine elevation (HP:0003348), urinary excretion of dicarboxylic acids (HP:0003215), and increased levels of long-chain acylcarnitine in plasma samples (HP:0045045). At 4 months, she showed a general worsening of her condition, with refusal to feed (HP:0011968), tachycardia (HP:0001649), and hepatomegaly (HP:0002240). An echocardiogram revealed a 15% reduction in the ejection fraction compared to her baseline (HP:0012664) plus systolic dysfunction (HP:0005185). After 10 days, she died. Her mother had polyhydramnios (HP:0001561) from the second trimester of gestation. All clinical and biochemical data are summarized in Table S1.

P2, the second daughter, debuted at 6 days of age with hypotonia (HP:0001319), lethargy (HP:0001254), hypoglycemia (HP:0001943), metabolic decompensation, hyperammonemia (HP:0001987), elevated transaminases (HP:0002910) and creatine kinase (HP:0003236). Analysis of metabolites in physiological fluids revealed high levels of lactic acid (HP:0003128) (3.7 mmol/mol of creatine normal value

around 2 mmol/mol), with metabolites of ketosis (HP:0002919), components of the Krebs cycle (succinate, fumarate, and 2-oxoglutarate [HP:0012401]), increased levels of alanine (values > 2× normal) (HP:0003348), plus long-chain acylcarnitine (C12-C18) (HP:0045045) and long-chain dicarboxylic acids (HP:0003215), all suggestive of a defect in fatty acid oxidation (FAO) or mitochondrial disease. At 15 days of age, P2 developed dilated cardiomyopathy (HP:0001644) like her elder sister. Dietary treatment with medium-chain fatty acids (Monogen[®], Nutricia) and carnitine was started, which notably improved her biochemical phenotype, restoring normal levels of acylcarnitine and amino acids, but succinate, fumarate, and 2-oxoglutarate remained elevated. At 4 months of age, after a bout of pneumonia (HP:0002090), her cardiac function deteriorated, manifested as contractility problems (HP:0006670) and episodes of tachycardia (HP:0006670). Very high levels of creatine kinase and liver dysfunction were also observed (HP:0001392). She died a few days later from cardiac (HP:0001635) and respiratory failure (HP:0002093). An anatomopathological study revealed she had suffered a myocardial infarction (Table S1).

2.2 | Genetic analysis

For genetic studies, DNA was extracted from peripheral blood using the MagnaPure system (Roche Applied Science). For P2, whole exome sequencing was performed using the Nextera DNA Exome Kit (Illumina).

Variant calling was undertaken using the DNAnexus bioinformatic pipeline. The overall mean target coverage was $61\times$, with a $>20\times$ base coverage of 77%. NGS data were analyzed for copy number variations using an in-house pipeline that compares the normalized mean coverage of targets between a patient and three control samples of the same pool. Sanger sequencing was used to confirm the presence of the identified variants and for testing Mendelian segregation, as well as to confirm the presence of the variants in the parents' samples and those of P1.

2.3 | Functional analysis of variants using patient-derived fibroblasts

P2 dermal-derived fibroblasts were grown under standard conditions in minimal essential medium containing 1 g/L of glucose supplemented with 2 mmol/L glutamine, 10% fetal bovine serum, and antibiotics. The cell lines CC2509 (Lonza) and GM8680 (Coriell Institute for Medical Research) were used as healthy controls.

PPCDC levels, and oligomerization of the trimer protein, were analyzed by Western blotting after SDS-PAGE and native-PAGE, respectively. Analysis of OxPhos complexes was performed in mitochondrial extracts. To that end, mitochondria were isolated using the hypotonic swelling procedure as described by ref. 19, and 15 μg of mitochondrial extract were incubated with 2% digitonin. The NativePAGE™ Novex® Bis-Tris Gel System (Invitrogen) was used (following the manufacturer's instructions) for the preparation of protein samples for native-PAGE. The primary polyclonal antibodies used were anti-PPCDC (1:250; PA5-61065, Thermo Fisher Scientific), anti-total OxPhos (CI-NDUFB8, CII-SDHB, CIII-UQCRC2, CIV-MTCOI, and CV-ATP5A) (ab110413; Abcam) at a dilution of 1:250, anti-NDUFA9 (1:500, ab14705), anti-SDHA (1:5000, ab14715), anti-MTCOI (1:1000, ab14705), and anti-ATP5A (1:2000, ab14748). Anti-tubulin (T9026, Sigma-Aldrich) and anti-citrate synthase (C5498, Sigma-Aldrich) at 1:1000 were used as loading controls.

pEZ-EX-I1642-Lv205 (GeneCopoeia) or pEZ-EX-I1642-M55 containing the complete open reading sequence of PPCDC (NM_021823.4), either alone or fused to mCherry protein, was used for the transient expression of PPCDC cDNA in fibroblasts. For this, 300 000 cells were seeded on p6 plates, or 700 000 on p60 plates, left for 24 h, and then transfected with 2 and 4 μg of DNA, respectively, using Lipofectamine™ LTX with PLUS™ reagent (Invitrogen) and OptiMEM. Cells were harvested 24–48 h after transfection or fixed on the plate for immunofluorescence assays.

For normal and mutant protein localization, the vector pEZ-EX-I1642-M55 containing PPCDC cDNA was used. Changes were introduced using the Quickchange™ Lightning Site-Directed Mutagenesis Kit (Agilent) following the supplier's recommendations. P2-derived and healthy control fibroblasts were transfected using 2 μg of the normal or mutant plasmid. The cells were then fixed with 10% formalin (Sigma-Aldrich) for 20 min at room temperature, permeabilized with 0.1% Triton X-100 in Tris-buffered saline (TBS) for 5 min, and then blocked for 30 min with blocking solution (0.3% donkey serum, 0.3% Triton X-100, TBS). Incubation with the primary antibody (anti-PPCDC, 1:50; anti-cytochrome C 1:500 [ab173529, Abcam]) was performed overnight at 4°C. Visualization was achieved using a secondary antibody with bound Alexa 488 or Alexa 555 (Thermo Fisher Scientific) at a concentration of 1:200 in blocking solution (left for 2 h at 37 °C). For nuclear staining, samples were incubated with DAPI (4',6-diamino-2-phenylindole) (Roche) at a concentration of 1:10 000 for 10 min, and then examined using an LSM710 confocal microscope coupled to an AxioImager M2 (Zeiss).

For the expression of PPCDC-interfering shRNA (PPCDC MISSION shRNA Bacterial Glycerol Stock—SHCLNG-NM_021823: TRCN0000155649, TRCN0000152453, TRCN0000154478, TRCN0000155901, and TRCN0000155902; Sigma-Aldrich), the plasmids were packaged in lentiviral particles for subsequent infection of the fibroblasts as previously described.²⁰

2.4 | Measurement of cellular ATP and CoA concentrations

ATP was extracted from healthy control and P2-derived fibroblasts grown in basal culture medium after incubation for 1 h with 100 mM 2-deoxy-D-glucose (2-DG) (Sigma-Aldrich) or 6 μM oligomycin (Invitrogen). ATP concentrations were measured using the luciferin-luciferase-based ATP Bioluminescence Assay Kit CLS II (Roche), following the manufacturer's instructions. The ATP concentration in each assay was normalized against the total protein concentration as determined by the Bradford method.

Total cellular CoA was measured using the Coenzyme A Assay Kit (Abcam) according to the manufacturer's instructions. Briefly, the cells were trypsinized and resuspended in 250 μl of lysis buffer without SDS (Mammalian Cell Lysis Buffer [Abcam]), incubated for 15 min at room temperature, and centrifuged at 1500g for 5 min. For each measurement, 50 μl of supernatant was used. CoA levels were determined by taking into account the number of cells present.

2.5 | Mitochondrial function

The oxygen consumption rate of control and P2-derived fibroblasts was measured using an XF24 Extracellular Flux Analyzer (Seahorse Bioscience, Izasa Scientific). MitoStress analysis was performed as described by ref. 19.

Electron microscopy imaging of control and P2-derived fibroblasts was performed as described by ref. 21 using a JEM1400 Flash (JEOL Ltd) electron microscope operating at 80 kV. Images were recorded with a 4k CMOS Oneview camera (Gatan). For the morphometric analysis of mitochondria, the major and minor axes of at least 100 randomly selected mitochondria were measured. The aspect ratio was defined as the major axis/minor axis ratio.²² The minimum aspect ratio of 1 corresponds to a perfect circle.

2.6 | Functional analysis of mutations in *Saccharomyces cerevisiae*

S. cerevisiae was grown at 28°C in YPD (1% yeast extract, 2% peptone, and 2% dextrose) or in a synthetic medium lacking uracil or leucine for plasmid selection. The synthetic medium was composed of 0.17% yeast nitrogen base (YNB) without ammonium sulfate or amino acids, 0.5% ammonium sulfate, 2% glucose, and 0.13% drop-out mix.²³ Growth tests were performed in drops as previously described,^{24,25} growing cells to saturation 72 h. Dilutions were made to OD₆₀₀ = 0.005 in fresh medium containing doxycycline and distributed in triplicate in 96-well plates (Thermo Fisher Scientific). A Synergy HTX multi-mode reader apparatus (Biotek) was used to monitor cell growth at 28°C by reading the OD₆₀₀ every 30 min for 88 h. Plates were shaken at low agitation over the entire experimental period.

The yeast strains used in this work were MAR24 (*MATa ura3-52 leu2-3112 trp1-1 his4 can-1r pteO-HAL3 vhs3::URA3*), MAR25 (*MATa/MATα ura3-52 leu2-3112 trp1-1 his4 can-1r CAB3/cab3::KANMX4*), and JA104 (*MATa ura3-52 leu2-3112 his4 trp1-1 can-1r hal3::LEU2*).^{13,15} To monitor the growth of strain MAR24 in liquid medium supplemented with doxycycline, and of JA104 in solid medium in the presence of LiCl, the strains were transformed with plasmids YCp111HAL3²⁶ or YEp195HAL3²⁷ (the latter providing the wild-type *HAL3* gene in a *URA3*-based high copy plasmid) or with the *S. cerevisiae HAL3* p.Thr53Pro (T302P) and p.Ala95Val (A385V) human-like variants. These changes were introduced into the YEp195HAL3 plasmid using the Quickchange™ Lightning Site-Directed Mutagenesis Kit (Agilent) following the supplier's instructions. For tetrad analysis, strain MAR25

was transformed with the centromeric plasmids bearing native Cab3 (YCp33-3FLAG-YKL088w) or its p.Thr53Pro (T347P) and p.Ala95Val (A398V) human-like variants. Sporulation and tetrad analysis procedures were performed as described in ref. 23. Figure S5 provides a flow-chart describing the functional tests performed in yeasts.

2.7 | Statistical analysis

Values are expressed as means or means ± SD of independently performed experiments. Differences between means were examined using the Student's *t* test. Significance was set at *p* < 0.05. All calculations were performed using GraphPad Prism 6 (GraphPad Software).

3 | RESULTS

Exome sequencing was performed in DNA from P2. A total of 34 967 variants were initially filtered based on their predicted consequences, and on a minor allele frequency (MAF) of 0.5% within the gnomAD database. A virtual phenotypic panel analysis was then undertaken using HPO terms, but the results were inconclusive. The filtered variants were then subjected to an agnostic analysis considering autosomal recessive inheritance. Variants potentially pathogenic or with unknown clinical significance (VUS), as assessed using the Varsome platform (<https://varsome.com/>), were prioritized by reducing the list to 23 variants (Table S2) in 15 different genes. Finally, two potential heterozygous single nucleotide variants (SNVs)—c.157A>C (p.Thr53Pro) and c.284C>T (p.Ala95Val)—of *PPCDC* were selected following the analysis in different databases of the functional role of each gene. These variants were either absent or present with a very low allelic frequency (c.284C>T; MAF: 0.0000319) in the gnomAD database and absent from the Collaborative Spanish Variant Server (CSVS). All mutation predictors indicated potential pathogenicity. Following ACMG criteria, p.Thr53Pro and p.Ala95Val were classified as VUS (codes PM2 andPP3). Mendelian segregation analysis of the parents' samples indicated c.157A>C and c.284C>T in the maternal and paternal alleles, respectively (Figure 2A). P1 was confirmed as a carrier of both variants. Both variants were present in similar amounts in the mRNA of P2-derived fibroblasts compared to healthy control fibroblasts. GeneMatcher detected no further issues of interest.

Sequence alignments against bacteria through to mice indicated the Thr53 and Ala95 residues (Figure 2B) to be strongly conserved. Based on the crystal structure of human *PPCDC*, possible functional effects for both

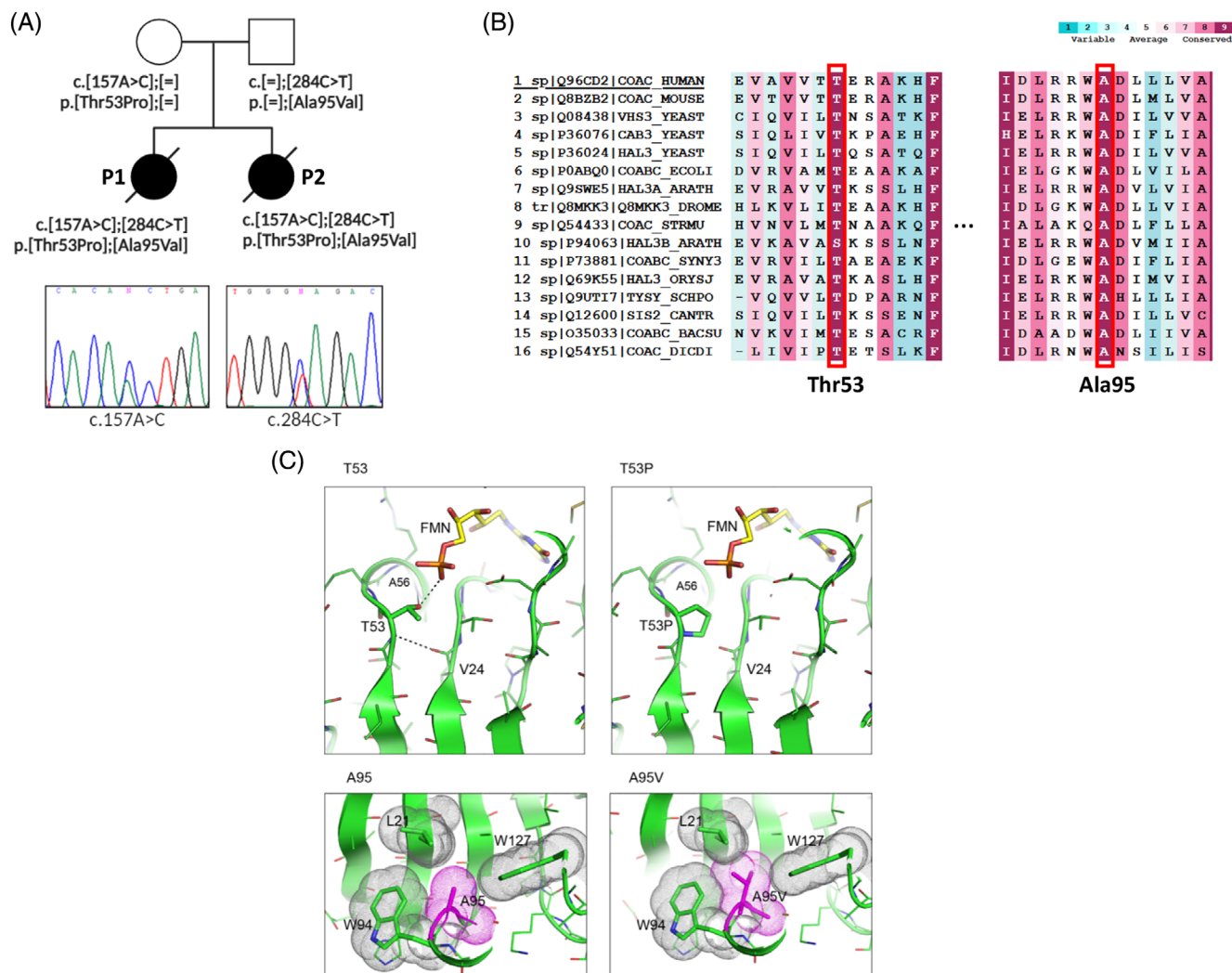


FIGURE 2 Identification of *PPCDC* variants and their possible harmful effects. (A) Pedigree and chromatogram of the *PPCDC* variants identified in P1 and P2. (B) Analysis of conservation and localization of variant *PPCDC*; protein sequence alignment with different species using the ConSurf Server. Color code in the upper panel. The amino acids corresponding to human Thr53 and Ala95 are marked with red squares. (C) Location of the substitutions p.Thr53Pro (T53P) and p.Ala95Val (A95V) in the *PPCDC* protein (PDB entry 1QZU), showing the natural amino acid (on the left) and the substitution (on the right). Hydrogen bonds are represented with dotted lines. The Van der Waals surface for Ala95 and the surrounding side chains is represented as dots. A56, Ala56; FMN, flavin mononucleotide.

pathogenic variants are proposed (Figure 2C). The side chain of residue Thr53 participates directly in the binding of the phosphate group of FMN and establishes an H-bond with the amino group of Ala56, stabilizing the first turn of the α -helix. In addition, the amino group of Thr53 makes an H-bond with the carbonyl oxygen of Val24, stabilizing the H-bonds in the β -strand that nucleates the protein. All of these interactions would be hampered by replacing Thr53 with a proline; thus, mutation p-Thr53Pro should reduce affinity for the essential cofactor FMN and likely cause protein folding and stability problems. In addition, the side chain of Ala95 is buried in a hydrophobic cavity formed by the side chains of residues Leu21, Trp94, and Trp127. The presence of a larger Val at this position would cause a steric hindrance difficult to

resolve given the limited mobility of the large Leu and Trp residues. Thus, mutation p.Ala95Val likely causes protein folding and stability problems.

The potential effects of the variants on the *PPCDC* protein were then examined. Steady-state protein was undetectable by Western blotting in P2-derived fibroblasts, while a 22 kDa protein was detected in the healthy control cells (Figure 3A). Antibodies detected a complex SDS-PAGE pattern, including a 22 kDa band present in the control but absent from the P2 protein extract that matched the predicted size of the *PPCDC* monomer (22 282 Da). Transfection of healthy control and P2-derived fibroblasts with wild-type *PPCDC* cDNA recovered the 22 kDa band (Figure S1). Similar results were obtained using native PAGE gels, which revealed a

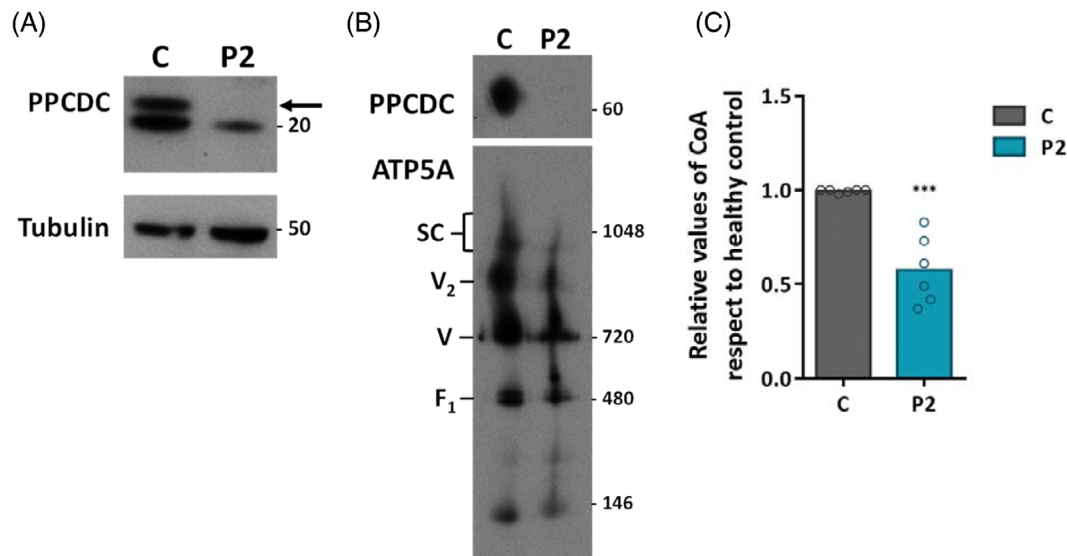


FIGURE 3 Western blot analysis and measurement of CoA levels in P2-derived fibroblasts. (A) Western blot following SDS-PAGE, and (B) native PAGE analysis of PPCDC in control fibroblasts (C) and P2-derived fibroblasts. Tubulin and ATP5A were used as loading controls. (C) Concentration of CoA in cell extracts from healthy control (C) and P2-derived fibroblasts determined using a fluorometric method (performed with six biological replicates). Student's *t* test analysis performed ($***p < 0.001$). The plotted data are normalized with respect to the control data in each experiment.

66 kDa protein corresponding to the expected homotrimer assembly in the healthy control; this was absent from the P2-derived fibroblasts (Figure 3B).

The expression and subcellular localization of native PPCDC and the p.Thr53Pro and p.Ala95Val variants were assessed by confocal microscopy in P2-derived fibroblast using N-terminal mCherry tagged constructs (Figure S2). PPCDC protein was detected in both healthy control and P2-derived fibroblasts always cytosolic and with no obvious differences in quantity. A different detection capacity of the antibodies used and/or the stabilizing effect of the mCherry label could explain the apparent discrepancy between the results of western blot and immunofluorescence analysis.

3.1 | Biochemical phenotyping of P2-derived fibroblasts

To gain further insight into the metabolic impact of PPCDC deficiency, CoA in cell extracts was determined fluorometrically. A significant (43%) reduction in CoA was seen in the P2-derived fibroblasts compared to healthy controls (Figure 3C).

Since a reduction in CoA would likely have different metabolic effects, mitochondrial respiration was studied in P2-derived fibroblasts grown under standard conditions (glucose), or in the presence of galactose (forcing the cell to obtain energy via mitochondrial respiration). Significant differences in respiratory variables were

observed between the healthy control and P2-derived fibroblasts (Figure 4). In the presence of galactose, a significant reduction was seen in the latter in terms of the maximum respiration (R_{max}) and the reserve capacity (Spare). However, ATP levels in these cells were significantly increased in the presence of glucose (Figure S3). The inhibition of glycolysis with 2'-deoxy-D-glucose led to a drastic decrease in intracellular ATP concentrations (Figure S3); thus, ATP production occurs via the glycolytic pathway rather than mitochondrial respiration.

Finally, mitochondrial ultrastructure was assessed via mitochondrial elongation (measuring the aspect ratio). No variation was seen in this respect, nor in the structure of the cristae between the control and P2-derived fibroblasts (Figure S4).

3.2 | Modeling the disease in PPCDC knock-down fibroblasts

A knock-down model of healthy, control fibroblasts was used to determine the impact of reducing PPCDC on total CoA. Five shRNAs directed against different regions of PPCDC were tested. The efficiency of their interference was verified by RT-qPCR (data not shown) and Western blotting (Figure 5A). sh3 and sh4 were selected to assess the silencing effect on CoA levels in cell extracts. Figure 5B shows that the CoA levels underwent a significant reduction of 26% for the sh3 model compared to the control shRNA, and 17% for sh4. These results reinforce

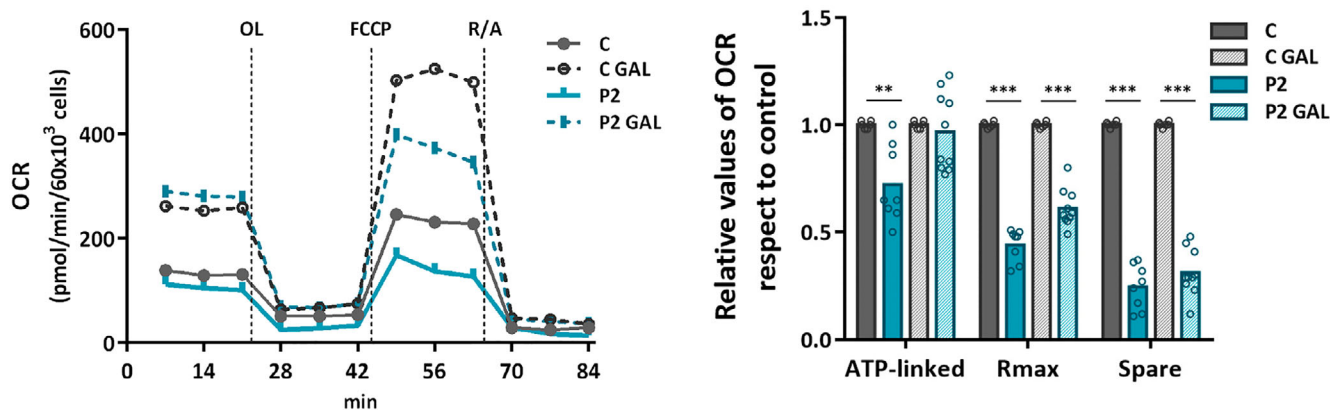


FIGURE 4 Mitochondrial respiration with glucose/galactose. Representative respiratory profile in healthy control (C) and P2-derived fibroblasts, in the presence of glucose (solid line) and galactose (dotted line), and after the consecutive addition of oligomycin 6 μ M (OL), FCCP 20 μ M (FCCP), rotenone and antimycin A 1 μ M (R/A). All data are the average of at least three biological replicates of experiments performed in triplicate-quintuplicate. Student's *t* test analysis performed (** $p < 0.01$; *** $p < 0.001$). Rmax, maximum respiration; Spare, reserve capacity.

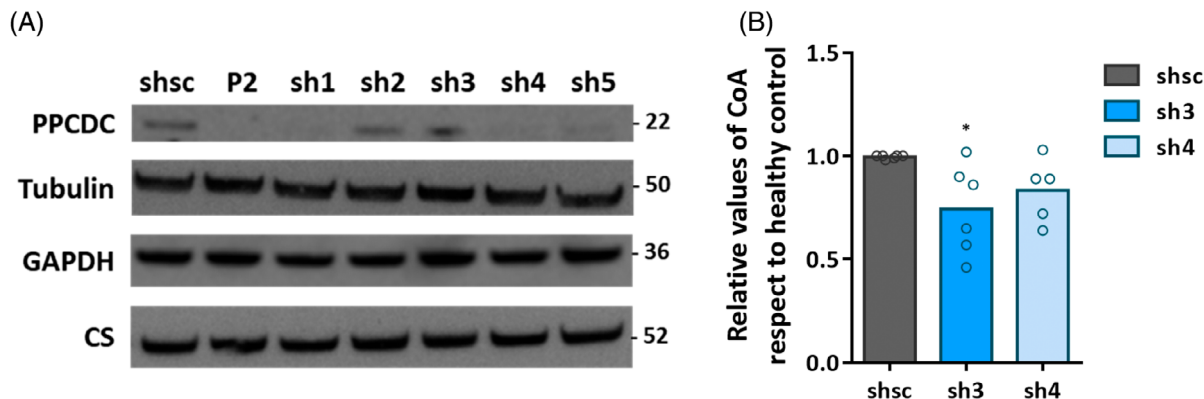


FIGURE 5 PPCDC knock-down cellular model. (A) PPCDC levels as determined by Western blotting following interference by the five shRNA, showing the results for two (sh3 and sh4). Tubulin and GAPDH were used as loading controls. Citrate synthase (CS) was used as a mitochondrial marker. (B) Cellular CoA levels after interference with sh3 and sh4. Data are from at least five experiments performed in triplicate. shsc, control shRNA; shx, 5 different shRNA. Student's *t* test analysis performed (* $p < 0.05$). The plotted data are normalized with respect to the control data in each experiment.

the P2-derived fibroblast data which revealed an almost complete absence of PPCDC in these cells, although the CoA levels were not drastically reduced.

3.3 | Phenotypic analysis of the specific mutations in a yeast model

To verify whether the p.Thr53Pro and p.Ala95Val variants identified in the human *PPCDC* gene impair its function and might be responsible for the clinical and biochemical phenotype observed in the patients, the yeast *S. cerevisiae* was used as a model (see flowchart in Figure S5 describing the functional tests performed). Overexpression of the Hal3 protein is known to confer

tolerance to toxic monovalent cations, such as LiCl, an effect derived from its capacity to inhibit the Ppz1 phosphatase. In the first instance, the growth behavior of the haploid strain JA104, which is defective in *HAL3*, after its transformation with multicopy plasmids bearing either native *Hal3* or its human-like p.Thr53Pro and p.Ala95Val variants, was assessed; this was performed on a solid medium with different concentrations of LiCl. A dramatic reduction in LiCl tolerance was detected in clones bearing either mutation compared to the wild-type (Figure S6).

The capacity of the variants to impair CoA synthesis was also tested by transforming yeast strain MAR24 (a conditional *hal3 vhs3* double mutant in which the *VHS3* gene is deleted and the *HAL3* promoter replaced

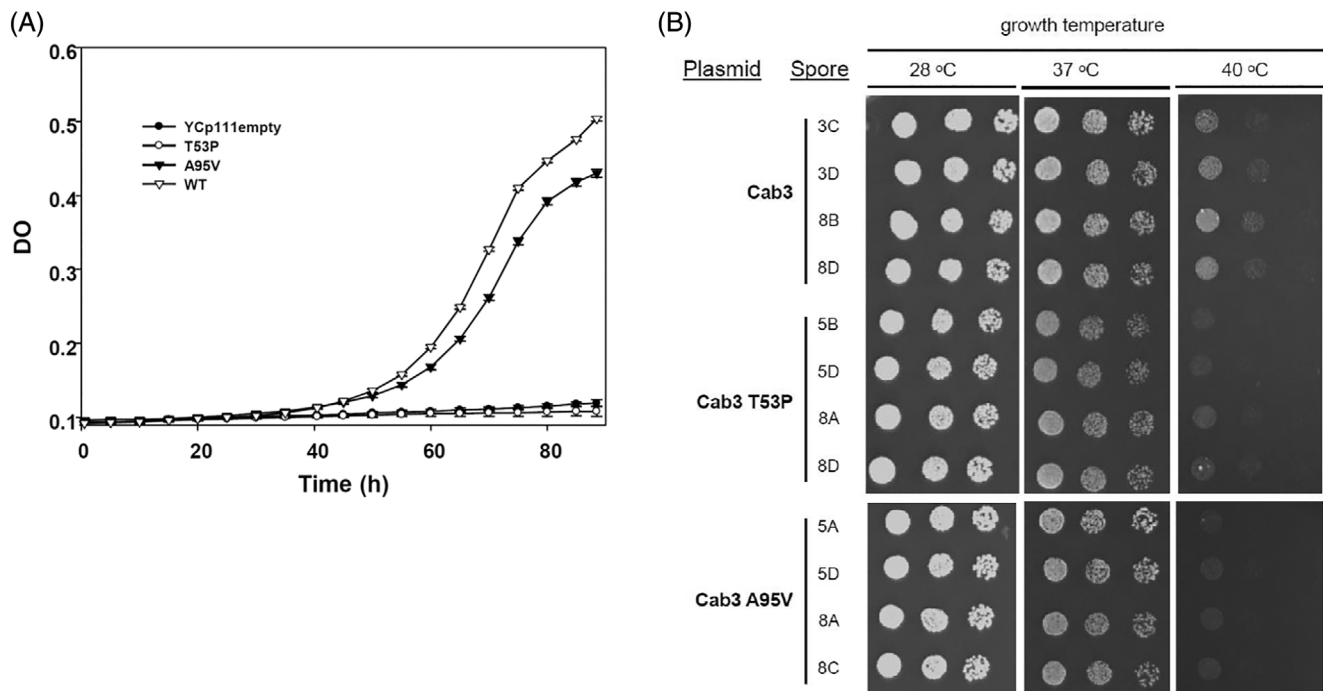


FIGURE 6 (A) Growth curves of the *Saccharomyces cerevisiae* strain MAR24. The haploid strain MAR24 (*tetO:hal3 vhs3*) was transformed with YCp111-based plasmid expressing either wild-type Hal3 (WT), its human-like p.Thr53Pro (T53P) and p.Ala95Val (A95V) variants, or the YCp111 empty plasmid as a negative control. Cells were grown in YNB medium with doxycycline at 28°C on a shaking platform. Data are means \pm SD. (B) A temperature-sensitive phenotype is conferred by the expression of the human-like p.Thr53Pro and p.Ala95Val Cab3 variants in *S. cerevisiae*. The diploid strain MAR25, heterozygous for the *cab3:KANMX4* deletion was transformed with centromeric plasmids bearing native Cab3 or its human-like p.Thr53Pro (T53P) and p.Ala95Val (A95V) variants. Cells were induced to sporulate and tetrad analysis was performed. Spores (haploid cells) from several tetrads were analyzed for the presence of the *CAB3* deletion and the plasmid. Cultures were spotted on plates of synthetic medium lacking uracil and grown at 28°C and 37°C for 3 days, or at 40°C for 5 days.

by a doxycycline-regulatable *tetO* promoter¹⁵) with the wild-type YCp111HAL3 plasmid, or the *HAL3* human-like p.Thr53Pro and p.Ala95Val variants. In YNB liquid medium supplemented with doxycycline, which strongly represses the expression of native *HAL3*,^{15,28} no growth was observed for clones with the yeast p.Thr53Pro variant, or for those transformed with YCp111 (empty vector). Clones bearing the human-like p.Ala95Val variant, however, while showing moderate growth delay, reached a final density of \sim 84% compared to the wild-type (Figure 6A). Because the lethality in yeast of the *hal3 vhs3* double mutation does not depend on Ppz1 activity,¹⁵ but on the inability of building up a functional PPCDC heterotrimer,¹³ these results suggest that the human-like p.Thr53Pro variant, and particularly the p.Ala95Val variant, in addition to their effect on Ppz1 regulation, might affect CoA synthesis.

To further test the effect of p.Thr53Pro and p.Ala95Val on CoA biosynthesis, plasmids bearing native Cab3 (essential for PPCDC activity) or its corresponding variants were introduced into the diploid heterozygous

strain MAR25, in which one of the alleles of *CAB3* is deleted. The cells were induced to sporulate, and tetrads were dissected to isolate viable haploid spores. Whereas cells transformed with the empty vector showed the characteristic 2:2 segregations (only two spores germinate), most tetrads carrying the native Cab3, or its mutated versions, gave rise to four viable spores (not shown). This indicates that, at least in part, the extrachromosomal material is able to rescue Cab3 deficiency. To better characterize the behavior of the mutated versions, viable haploid clones with the *CAB3* deletion were grown and tested for a temperature-sensitivity phenotype. Figure 6B shows that clones bearing the p.Thr53Pro variant grew slightly worse than the wild-type at 37°C; at 40°C reduced growth was clearly observed for clones expressing either the p.Thr53Pro or p.Ala95Val human-like variants of Cab3. These results suggest that the mutated versions are associated with a temperature-sensitive phenotype, implying some degree of structural destabilization and that this defect is stronger for the p.Thr53Pro variant.

4 | DISCUSSION

Massive parallel sequencing in combination with functional genomics represents an undeniable advance in diagnosing patients with severe, ultra-rare diseases. The ability to identify patients with defects in genes never associated with any pathology not only provides insight into cellular metabolism, but also offers clues regarding early treatments that might help avoid organ damage. The present work describes variants of *PPCDC*, one of the four genes involved in the synthesis of CoA in humans, that are associated with an ultra-rare form of autosomal recessive, dilated cardiomyopathy.

Whole exome sequencing identified *PPCDC* biallelic variants in two sisters. The strong conservation of the affected residues suggested these variants to be harmful. Computational analysis indicated that variants p-Thr53Pro and p.Ala95Val would likely affect protein folding and stability, and also, the p.Thr53Pro would predictably affect the binding of FMN. The potential pathogenic effect correlates with the absence of steady levels of *PPCDC* protein in P2-derived fibroblasts. However, while the two cellular models of disease (patient-derived fibroblasts and the knock-down model) produced no detectable protein, CoA was not completely absent (a reduction of 43% was detected in patient-derived fibroblast and a decrease of 17%–25% in the knock-down model). Such apparent discrepancies have also been described for other defects impacting the CoA synthesis pathway (such as those in *PPCS*, *PKAN2*, or *COASY*)¹⁰ and can be justified by two alternative and non-exclusive explanations: that the mutant proteins retain some residual activity and/or that cells might synthesize CoA from exogenous 4'-phosphopantetheine.^{3,5} Such alternative routes could help maintain the CoA pool in cultured cells.²⁹ Recent studies associate the PI3K pathway with the regulation of de novo CoA synthesis,³⁰ highlighting the different regulatory mechanisms that could be controlling this pathway. Thus, phenotypes induced by intracellular CoA reduction can be reversed when exogenous CoA is provided except in *COASY* defects due to the need for its activity to convert 4'-phosphopantetheine to CoA.

After a VUS variant is identified, a functional assessment is required to determine the relationship between the genotype and the phenotype. The present work reveals the pathogenicity of the studied variants and their possible effects via the use of a yeast model. The complete lack of *PPCDC* function in *S. cerevisiae* is lethal, and *PPCDC* activity requires the presence of Cab3 and either Hal3 or Vhs3. Neither of the studied human variants allowed for normal growth when the corresponding yeast genes were expressed in conditional *hal3 vhs3* mutants or

cab3 mutants. In fact, the temperature-sensitive loss of function of both Cab3 variants suggests that these mutations result in a less stable protein, an observation that fits well with the undetectable levels observed in the derived fibroblast models.

To date, two types of clinical phenotypes have been associated with deficiencies in this pathway. Patients with defects in *PANK2* and *COASY* manifest an early onset neurodegenerative pathology,^{8,31} while those with mutations in *PPCS* (identified in five individuals from unrelated families) show different degrees of dilated cardiomyopathy but no neurodegenerative symptoms.¹⁰ Both present patients had dilated cardiomyopathy, lactic acidosis, and long-chain acylcarnitine as well as the more severe form of *PPCS*-affected patient (Table S3). In both defects, low CoA levels in the heart might be related to this. It is worth noting that in bacteria both *PPCS* and *PPCDC* activities are combined into a bifunctional CoaBC protein, which in *Mycobacterium tuberculosis* has been shown to form an oligomeric complex.³² In addition, it has been proposed that, in yeast, the CoA biosynthesis enzymes (except pantothenate kinase Cab1) associate in a CoA synthesizing complex (CoA-SPC) with Cab3 as a nuclear component.³³ It is tempting to hypothesize that the strong effects of *PPCS* and *PPCDC* deficiency in humans, with particular emphasis in tissues (such as the heart) with high energy requirements, could be related to the formation of the core of a larger CoA-synthesizing protein complex. Further analysis in cardiomyocyte-derived iPSC will provide insight into the specific phenotype and the cardiac function affected.

Both present patients debuted in the neonatal period with clinical and biochemical phenotypes compatible with impairment of FAO. In fact, the metabolic signature of these patients involved increased levels of acylcarnitine and long-chain dicarboxylic acylcarnitine (C14 and C16). This biochemical phenotype is similar to that described for some mitochondrial β -oxidation-associated defects, such as Carnitine palmitoyltransferase 2 (MIM#600649) and Very long-chain acyl-CoA dehydrogenase (MIM#201475) deficiencies.³⁴ It has also been described in *Pank1*^{-/-} mice with defects in the hepatic enzyme pantothenate kinase 1 (*PANK1*).³⁵ Indeed, the biochemical signatures were consistent with a possible reduction in intracellular CoA that could possibly have led to a reduced synthesis of activated long-chain fatty acids.¹⁰ The determinations of total CoA would seem to corroborate the hypothesis of a possible reduction in intracellular CoA. This would be more significant in a cellular compartment with higher requirements, such as the mitochondria.

The loss of maximal respiratory capacity and the high levels of total ATP measured in the P2-derived fibroblasts in the presence of glucose would seem to indicate an increase

in the use of the glycolytic pathway to produce energy. In summary, the values for the biochemical variables measured in physiological fluids and patient-derived fibroblasts would appear to indicate a mitochondrial defect associated with a reduced capacity to catabolize fatty acids.

CoA and its derivatives play a central role in regulating cardiac energy metabolism since the heart's principal energy source comes from the oxidation of fatty acids and a lesser extent from glucose.³⁶ Based on this hypothesis, the phenotype and outcome of patients with higher CoA requirements should be experiencing more severe cardiac alterations.

Both patients died in the first year of life; no treatment was possible. However, based on the promising results obtained with a *Drosophila* PPCS model,¹⁰ the very early detection of these pathologies might allow for 4'-phosphopantothene supplementation with the aim of bypassing PPCDC deficiency. Genomic screening of newborns would allow for the implementation of personalized treatments for those who require it.³⁷

In summary, this work identifies variants in *PPCDC* that cause an ultra-rare metabolic disease affecting the CoA synthesis pathway. These are the first variants of this gene to be associated with human disease.

ACKNOWLEDGMENTS

This work was funded by the Instituto de Salud Carlos (ISCIII), the European Regional Development Fund [PI19/01155], the Ministerio de Economía, Industria y Competitividad, Spain (BFU2017-82574-P), and the Consejería de Educación, Juventud y Deporte, Comunidad de Madrid [B2017/BMD3721].

CONFLICT OF INTEREST

The authors declare no conflict of interest.

DATA AVAILABILITY STATEMENT

Data archiving is not mandated but data will be made available on reasonable request.

ETHICS STATEMENT

All procedures followed were in accordance with the ethical standards of the responsible committee on human experimentation (institutional and national) and with the Helsinki Declaration of 1975, as revised in 2000. This study was approved by Universidad Autónoma de Madrid Ethics Committee. Written informed consent was obtained from the parents of the patients for collection of samples and publication of medical data.

ORCID

Belén Pérez  <https://orcid.org/0000-0002-3190-1958>

REFERENCES

1. Strauss E. 7.11 – Coenzyme A biosynthesis and enzymology. In: Liu HW(B), Mander L, eds. *Comprehensive Natural Products II*. Elsevier; 2010:351-410. doi:10.1016/B978-008045382-8.00141-6
2. Lambrechts RA, Schepers H, Yu Y, et al. CoA-dependent activation of mitochondrial acyl carrier protein links four neurodegenerative diseases. *EMBO mol Med*. 2019;11(12):e10488. doi:10.15252/emmm.201910488
3. de Villiers M, Strauss E. Metabolism: jump-starting CoA biosynthesis. *Nat Chem Biol*. 2015;11(10):757-758. doi:10.1038/nchembio.1912
4. Baković J, López Martínez D, Nikolaou S, et al. Regulation of the CoA biosynthetic complex assembly in mammalian cells. *Int J Mol Sci*. 2021;22(3):1131. doi:10.3390/ijms22031131
5. Srinivasan B, Baratashvili M, van der Zwaag M, et al. Extracellular 4'-phosphopantetheine is a source for intracellular coenzyme A synthesis. *Nat Chem Biol*. 2015;11(10):784-792. doi:10.1038/nchembio.1906
6. Hartig MB, Hörtnagel K, Garavaglia B, et al. Genotypic and phenotypic spectrum of PANK2 mutations in patients with neurodegeneration with brain iron accumulation. *Ann Neurol*. 2006;59(2):248-256. doi:10.1002/ana.20771
7. Zhou B, Westaway SK, Levinson B, Johnson MA, Gitschier J, Hayflick SJ. A novel pantothenate kinase gene (PANK2) is defective in Hallervorden-Spatz syndrome. *Nat Genet*. 2001; 28(4):345-349. doi:10.1038/ng572
8. Dusi S, Valletta L, Haack TB, et al. Exome sequence reveals mutations in CoA synthase as a cause of neurodegeneration with brain iron accumulation. *Am J Hum Genet*. 2014;94(1):11-22. doi:10.1016/j.ajhg.2013.11.008
9. Hayflick SJ, Kurian MA, Hogarth P. Chapter 19 – Neurodegeneration with brain iron accumulation. In: Geschwind DH, Paulson HL, Klein C, eds. *Handbook of Clinical Neurology*. Neurogenetics, Part I. Vol 147. Elsevier; 2018:293-305. doi:10.1016/B978-0-444-63233-3.00019-1
10. Iuso A, Wiersma M, Schüller HJ, et al. Mutations in PPCS, encoding phosphopantothienoylcysteine synthetase, cause autosomal-recessive dilated cardiomyopathy. *Am J Hum Genet*. 2018;102(6):1018-1030. doi:10.1016/j.ajhg.2018.03.022
11. Strauss E, Zhai H, Brand LA, McLafferty FW, Begley TP. Mechanistic studies on phosphopantothienoylcysteine decarboxylase: trapping of an enethiolate intermediate with a mechanism-based inactivating agent. *Biochemistry*. 2004;43(49):15520-15533. doi:10.1021/bi048340a
12. Kachroo AH, Vandeloo M, Greco BM, Abdullah M. Humanized yeast to model human biology, disease and evolution. *Dis Model Mech*. 2022;15(6):dmm049309. doi:10.1242/dmm.049309
13. Ruiz A, González A, Muñoz I, et al. Moonlighting proteins Hal3 and Vhs3 form a heteromeric PPCDC with Ykl088w in yeast CoA biosynthesis. *Nat Chem Biol*. 2009;5(12):920-928. doi:10.1038/nchembio.243
14. de Nadal E, Clotet J, Posas F, Serrano R, Gomez N, Ariño J. The yeast halotolerance determinant Hal3p is an inhibitory subunit of the Ppz1p ser/Thr protein phosphatase. *Proc Natl Acad Sci U S A*. 1998;95(13):7357-7362. doi:10.1073/pnas.95.13.7357
15. Ruiz A, Muñoz I, Serrano R, González A, Simón E, Ariño J. Functional characterization of the *Saccharomyces cerevisiae* VHS3 gene: a regulatory subunit of the Ppz1 protein phosphatase with

- novel, phosphatase-unrelated functions. *J Biol Chem.* 2004; 279(33):34421-34430. doi:[10.1074/jbc.M400572200](https://doi.org/10.1074/jbc.M400572200)
16. Clotet J, Garí E, Aldea M, Ariño J. The yeast ser/thr phosphatases sit4 and ppz1 play opposite roles in regulation of the cell cycle. *Mol Cell Biol.* 1999;19(3):2408-2415. doi:[10.1128/MCB.19.3.2408](https://doi.org/10.1128/MCB.19.3.2408)
 17. Di Como CJ, Bose R, Arndt KT. Overexpression of SIS2, which contains an extremely acidic region, increases the expression of SWI4, CLN1 and CLN2 in sit4 mutants. *Genetics.* 1995;139(1): 95-107. doi:[10.1093/genetics/139.1.95](https://doi.org/10.1093/genetics/139.1.95)
 18. Ferrando A, Kron SJ, Rios G, Fink GR, Serrano R. Regulation of cation transport in *Saccharomyces cerevisiae* by the salt tolerance gene HAL3. *Mol Cell Biol.* 1995;15(10):5470-5481. doi:[10.1128/MCB.15.10.5470](https://doi.org/10.1128/MCB.15.10.5470)
 19. Bravo-Alonso I, Navarrete R, Vega AI, et al. Genes and variants underlying human congenital lactic acidosis—from genetics to personalized treatment. *J Clin Med.* 2019;8(11):1811. doi:[10.3390/jcm8111811](https://doi.org/10.3390/jcm8111811)
 20. Bravo-Alonso I, Oyarzabal A, Sánchez-Aragó M, et al. Dataset reporting BCKDK interference in a BCAA-catabolism restricted environment. *Data Brief.* 2016;7:755-759. doi:[10.1016/j.dib.2016.03.038](https://doi.org/10.1016/j.dib.2016.03.038)
 21. Oyarzabal A, Bravo-Alonso I, Sánchez-Aragó M, et al. Mitochondrial response to the BCKDK-deficiency: some clues to understand the positive dietary response in this form of autism. *Biochim Biophys Acta.* 2016;1862(4):592-600. doi:[10.1016/j.bbdis.2016.01.016](https://doi.org/10.1016/j.bbdis.2016.01.016)
 22. De Vos KJ, Allan VJ, Grierson AJ, Sheetz MP. Mitochondrial function and actin regulate dynamin-related protein 1-dependent mitochondrial fission. *Curr Biol.* 2005;15(7):678-683. doi:[10.1016/j.cub.2005.02.064](https://doi.org/10.1016/j.cub.2005.02.064)
 23. Adams A, Gottschling DE, Kaiser CA, Stearns T. *Methods in Yeast Genetics: A Cold Spring Harbor Laboratory Course Manual.* Cold Spring Harbor Laboratory Press; 1998.
 24. Calafi C, López-Malo M, Velázquez D, et al. Overexpression of budding yeast protein phosphatase Ppz1 impairs translation. *Biochim Biophys Acta Mol Cell Res.* 2020;1867(8):118727. doi:[10.1016/j.bbamcr.2020.118727](https://doi.org/10.1016/j.bbamcr.2020.118727)
 25. Morín M, Bryan KE, Mayo-Merino F, et al. In vivo and in vitro effects of two novel gamma-actin (ACTG1) mutations that cause DFNA20/26 hearing impairment. *Hum Mol Genet.* 2009; 18(16):3075-3089. doi:[10.1093/hmg/ddp249](https://doi.org/10.1093/hmg/ddp249)
 26. Aksenova A, Muñoz I, Volkov K, Ariño J, Mironova L. The HAL3-PPZ1 dependent regulation of nonsense suppression efficiency in yeast and its influence on manifestation of the yeast prion-like determinant [ISP(+)]. *Genes Cells.* 2007;12(4):435-445. doi:[10.1111/j.1365-2443.2007.01064.x](https://doi.org/10.1111/j.1365-2443.2007.01064.x)
 27. Muñoz I, Ruiz A, Marquina M, Barceló A, Albert A, Ariño J. Functional characterization of the yeast Ppz1 phosphatase inhibitory subunit Hal3: a mutagenesis study. *J Biol Chem.* 2004;279(41):42619-42627. doi:[10.1074/jbc.M405656200](https://doi.org/10.1074/jbc.M405656200)
 28. Simón E, Clotet J, Calero F, Ramos J, Ariño J. A screening for high copy suppressors of the sit4 hal3 synthetically lethal phenotype reveals a role for the yeast Nha1 antiporter in cell cycle regulation. *J Biol Chem.* 2001;276(32):29740-29747. doi:[10.1074/jbc.M101992200](https://doi.org/10.1074/jbc.M101992200)
 29. Jeong SY, Hogarth P, Placzek A, et al. 4'-Phosphopantetheine corrects CoA, iron, and dopamine metabolic defects in mammalian models of PKAN. *EMBO Mol Med.* 2019;11(12):e10489. doi:[10.15252/emmm.201910489](https://doi.org/10.15252/emmm.201910489)
 30. Dibble CC, Barritt SA, Perry GE, et al. PI3K drives the de novo synthesis of coenzyme A from vitamin B5. *Nature.* 2022; 608(7921):192-198. doi:[10.1038/s41586-022-04984-8](https://doi.org/10.1038/s41586-022-04984-8)
 31. Leoni V, Strittmatter L, Zorzi G, et al. Metabolic consequences of mitochondrial coenzyme A deficiency in patients with PANK2 mutations. *Mol Genet Metab.* 2012;105(3):463-471. doi:[10.1016/j.ymgme.2011.12.005](https://doi.org/10.1016/j.ymgme.2011.12.005)
 32. Mendes V, Green SR, Evans JC, et al. Inhibiting *Mycobacterium tuberculosis* CoaBC by targeting an allosteric site. *Nat Commun.* 2021;12(1):143. doi:[10.1038/s41467-020-20224-x](https://doi.org/10.1038/s41467-020-20224-x)
 33. Olzhausen J, Moritz T, Neetz T, Schüller HJ. Molecular characterization of the heteromeric coenzyme A-synthesizing protein complex (CoA-SPC) in the yeast *Saccharomyces cerevisiae*. *FEMS Yeast Res.* 2013;13(6):565-573. doi:[10.1111/1567-1364.12058](https://doi.org/10.1111/1567-1364.12058)
 34. Yamada K, Taketani T. Management and diagnosis of mitochondrial fatty acid oxidation disorders: focus on very-long-chain acyl-CoA dehydrogenase deficiency. *J Hum Genet.* 2019; 64(2):73-85. doi:[10.1038/s10038-018-0527-7](https://doi.org/10.1038/s10038-018-0527-7)
 35. Leonardi R, Rehg JE, Rock CO, Jackowski S. Pantothenate kinase 1 is required to support the metabolic transition from the fed to the fasted state. *PLoS One.* 2010;5(6):e11107. doi:[10.1371/journal.pone.0011107](https://doi.org/10.1371/journal.pone.0011107)
 36. Abo Alrob O, Lопасchuk GD. Role of CoA and acetyl-CoA in regulating cardiac fatty acid and glucose oxidation. *Biochem Soc Trans.* 2014;42(4):1043-1051. doi:[10.1042/BST20140094](https://doi.org/10.1042/BST20140094)
 37. Holm IA, Agrawal PB, Ceyhan-Birsoy O, et al. The BabySeq project: implementing genomic sequencing in newborns. *BMC Pediatr.* 2018;18(1):225. doi:[10.1186/s12887-018-1200-1](https://doi.org/10.1186/s12887-018-1200-1)

SUPPORTING INFORMATION

Additional supporting information can be found online in the Supporting Information section at the end of this article.

How to cite this article: Bravo-Alonso I, Morin M, Arribas-Carreira L, et al. Pathogenic variants of the coenzyme A biosynthesis-associated enzyme phosphopantothoenoylcysteine decarboxylase cause autosomal-recessive dilated cardiomyopathy. *J Inherit Metab Dis.* 2023;1-12. doi:[10.1002/jimd.12584](https://doi.org/10.1002/jimd.12584)